Chapter 4
Planar Parallel Robotic Machine Design

4.1 Preamble

Parallel kinematic machines with their unique characteristics of high stiffness (their actuators bear no moment loads but act in a simple tension or compression) and high speeds and feeds (high stiffness allows higher machining speeds and feeds while providing the desired precision, surface finish, and tool life), combined with versatile contouring capabilities have made parallel mechanisms the best candidates for the machine tool industry to advance machining performance. It is noted that the stiffness is the most important factor in machine tool design since it affects the precision of machining. Therefore, to build and study a general stiffness model is a very important task for machine tool design. In this chapter, we will build a general stiffness model through the approach of kinematic and static equations. The objective of this model is to provide an understanding of how the stiffness of the mechanism changes as a function of its position and as a function of the characteristics of its components. This can be accomplished using stiffness mapping.

There are two methods to build mechanism stiffness models [170]. Among them, the method which relies on the calculation of the parallel mechanism's Jacobian matrix is adopted in this book.

It will be shown that the stiffness of a parallel mechanism is dependent on the joint's stiffness, the leg's structure and material, the platform and base stiffness, the geometry of the structure, the topology of the structure, and the end-effector position and orientation.

Since stiffness is the force corresponding to coordinate i required to produce a unit displacement of coordinate j, the stiffness of a parallel mechanism at a given point of its workspace can be characterized by its stiffness matrix. This matrix relates the forces and torques applied at the gripper link in Cartesian space to the corresponding linear and angular Cartesian displacements. It can be obtained using kinematic and static equations. The parallel mechanisms considered here are such that the velocity relationship can be written as in (4.1),

$$\dot{\theta} = \mathbf{J}\dot{\mathbf{x}}, \tag{4.1}$$

D. Zhang, *Parallel Robotic Machine Tools*, DOI 10.1007/978-1-4419-1117-9_4,

where $\dot{\theta}$ is the vector of joint rates and $\dot{\mathbf{x}}$ is the vector of Cartesian rates – a six-dimensional twist vector containing the velocity of a point on the platform and its angular velocity. Matrix $\mathbf{J}$ is usually termed Jacobian matrix, and it is the mapping from the Cartesian velocity vector to the joint velocity vector. From (4.1), one can conclude that

$$\delta\theta = \mathbf{J}\delta\mathbf{x}, \tag{4.2}$$

where $\delta\theta$ and $\delta\mathbf{x}$ represent joint and Cartesian infinitesimal displacements, respectively. Then, one can get the stiffness of this mechanism using the principle of kinematic/static duality. The forces and moments applied at the gripper under static conditions are related to the forces or moments required at the actuators to maintain the equilibrium by the transpose of the Jacobian matrix $\mathbf{J}$. This is also true for parallel mechanism [**?**], and one can then write

$$\mathbf{F} = \mathbf{J}^T\mathbf{f}, \tag{4.3}$$

where $\mathbf{f}$ is the vector of actuator forces or torques, and $\mathbf{F}$ is the generalized vector of Cartesian forces and torques at the gripper link, which is also called the wrench acting at this link [14, 165]. The actuator forces and displacements can be related by Hooke's law, one has

$$\mathbf{f} = \mathbf{K}_J\delta\theta \tag{4.4}$$

with $\mathbf{K}_\mathrm{J} = \mathrm{diag}[k_1, \ldots, k_n]$, where each of the actuators in the parallel mechanism is modeled as an elastic component, $\mathbf{K}_\mathrm{J}$ is the joint stiffness matrix of the parallel mechanism, k_i is a scalar representing the joint stiffness of each actuator, which is modeled as linear spring, and the ith component of vector $\mathbf{f}$, noted f_i is the force or torque acting at the ith actuator. Substituting (4.2) into (4.4), one obtains

$$\mathbf{f} = \mathbf{K}_\mathrm{J}\mathbf{J}\delta\mathbf{x}. \tag{4.5}$$

Then, substituting (4.5) into (4.3), yields

$$\mathbf{F} = \mathbf{J}^\mathrm{T}\mathbf{K}_\mathrm{J}\mathbf{J}\delta\mathbf{x}. \tag{4.6}$$

Hence, $\mathbf{K}_\mathrm{C}$, the stiffness matrix of the mechanism in the Cartesian space is then given by the following expression

$$\mathbf{K}_\mathrm{C} = \mathbf{J}^\mathrm{T}\mathbf{K}_J\mathbf{J}. \tag{4.7}$$

Particularly, in the case for which all the actuators have the same stiffnesses, i.e., $k_1 = k_2 = \cdots = k_n$, then (4.7) will be reduced to

$$\mathbf{K} = k\mathbf{J}^\mathrm{T}\mathbf{J}, \tag{4.8}$$

which is the equation given in [57].

The stiffness matrix is a positive semidefinite symmetric matrix whose eigenvalues represent the coefficients of stiffness in the principal directions, which are given by the eigenvectors. These directions are in fact represented by twist vectors, i.e., generalized velocity vectors. Moreover, the square root of the ratio of the smallest eigenvalue to the largest one gives the reciprocal of the condition number κ of the Jacobian matrix [83], which is a measure of the dexterity of the mechanism [56]. It can be written as

$$\frac{1}{\kappa} = \sqrt{\frac{\lambda_{\min}}{\lambda_{\max}}}, \tag{4.9}$$

where $\lambda_{\min}$ and $\lambda_{\max}$ are the smallest and largest eigenvalues of the stiffness matrix, respectively.

From (4.7), it is clear that if the Jacobian matrix of a mechanism $\mathbf{J}$ is singular, then obviously, the stiffness matrix of the mechanism, $\mathbf{J}^T\mathbf{K}_J\mathbf{J}$ is also singular, thus the mechanism loses stiffness, there is no precision also for the mechanism. Hence, one can study the precision of machine tools through their stiffness model, and then find the most suitable designs.

The flexibilities included in the model can be classified in two types [36] 1) the flexibilities at the joints and 2) the flexibilities of the links. Hence, the complete lumped model should include the following three submodels:

- The *Denavit–Hartenberg model* which defines the nominal geometry of each of the kinematic chains of the mechanism, the kinematics described by the Denavit–Hartenberg matrix are straightforward and systematic for mechanisms with rigid links. They are also effective for mechanisms with flexible links
- *A lumped joint model* which is defined in Table 4.1
- *An equivalent beam model* at each link which accounts for the deformations of the link caused by the external forces and torques

In order to simplify the model of the stiffness, link stiffnesses will be lumped into local compliant elements (spring) located at the joints. This is justified by the fact that no dynamics is included in the model (it is purely kinematic) and that limited numerical accuracy is acceptable. Indeed, the objective of this study is to obtain engineering values for the stiffness and to determine which areas of the workspace lead to better stiffness properties.

Physically, the bending deformation in joints is presented in different ways. In the planar case, the unactuated revolute joint does not induce any bending whereas in the spatial case, a bending is presented in a direction perpendicular to the joint. Hence, it is necessary to establish a lumped joint model for each possible case. In the lumped joint model, deformations caused by link flexibility can be considered as virtual joints fixed at this point; the details are given in [62] and Table 4.1.

A linear beam is shown in Fig. 4.1, where F is the external force, E the elastic modulus, L the length of the beam, and I is the section moment of inertia of the beam. In a lumped model, the flexible beam will be replaced by a rigid beam mounted on a pivot plus a torsional spring located at the joint, as illustrated in Fig. 4.1b. The objective is to determine the equivalent torsional spring stiffness that

Table 4.1 Lumped joint models for planar system

Joint type	If actuated, the equivalent model	If unactuated, the equivalent model
Revolute	2 Torsional springs 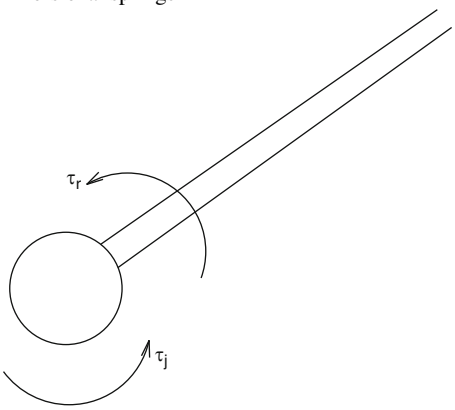	No bending
Prismatic	Actuated spring 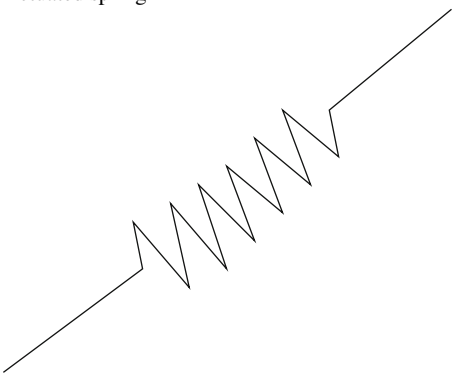	Uncertainty

will produce the same tip deflection as that of the beam under the load F. As it can be seen on the figure, the lumped model will lead to a different orientation of the tip of the beam. However, assuming that the deformation is small, angle θ will also be small, thus the difference in orientation between the original beam and the equivalent link can be neglected. Moreover, since in the mechanisms considered here, the legs are attached to the platform with spherical joints, there is not any moment presented at the spherical joint, hence, the end link orientation of the beam is irrelevant. Let δ be the deflection of the beam. Based on the Castiliano's theorem [143], one can build an equivalent rigid beam model based solely on the deflection of the free end. With a force F applied at the free end of the beam, the resulting deformation can be written as (see Fig. 4.1a)

$$\delta = \frac{FL^3}{3EI} \tag{4.10}$$

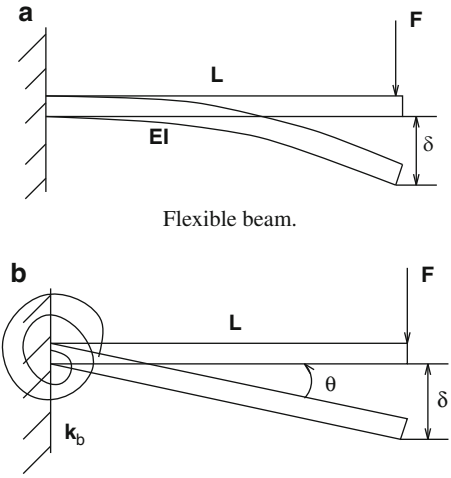

Fig. 4.1 Link deformation induced by wrench

and assuming small deformations, the corresponding rotational deformation of an equivalent rigid beam with a torsional spring would be

$$\theta \simeq \frac{\delta}{L}. \tag{4.11}$$

Let the deflection in both cases (Fig. 4.1a, 4.1b) be the same. Substituting (4.10) into (4.11), yields

$$\theta = \frac{FL^2}{3EI}, \tag{4.12}$$

where δ is the flexible beam's deflection at the free end and θ is the rigid beam's rotation around the joint.

Since the flexible beam model can be lumped into a torsional spring with equivalent stiffness k_b at the shoulder joint (Fig. 4.1b), based on the principle of work and energy, one has

$$\frac{1}{2}F\delta = \frac{1}{2}k_\mathrm{b}(\theta)^2, \tag{4.13}$$

where k_b is the lumped stiffness of the flexible beam. Substituting (4.11) to (4.13), one obtains

$$FL\theta = k_\mathrm{b}\theta^2 \tag{4.14}$$

or

$$k_\mathrm{b} = \frac{FL}{\theta}. \tag{4.15}$$

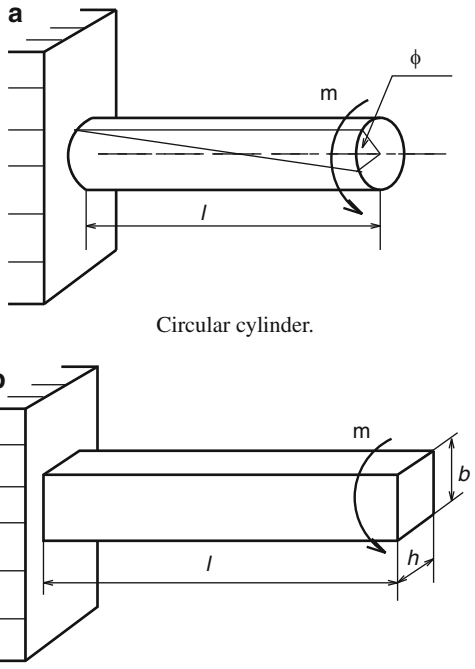

Fig. 4.2 Link deformation induced by torque

Substituting (4.12) into (4.15), one obtains the equivalent stiffness for the flexible beam as

$$k_{\mathrm{b}} = \frac{3EI}{L}. \tag{4.16}$$

Here the lumped stiffness expression for a single flexible beam undergoing twisting is addressed. A linear beam is shown in Fig. 4.2, where m(Nm) is the external torque, $G\,(\mathrm{N/m^2})$ the shear elastic modulus, l(m) the length of the beam, and $I\,(\mathrm{m^4})$ is the section moment of inertia of the beam. Similarly to the preceding section, the flexible beam is replaced by a rigid beam mounted at the end plus a torsional spring located at the end. The objective is to determine the equivalent torsional spring stiffness that will produce the same tip deflection as that of the beam under the load m. Assuming that the deformation is small, angle ϕ will also be small, then, with a twist m applied at the free end of the beam, the resulting deformation can be written as

$$\Delta\phi = \frac{ml}{GI} \quad \text{for circular cylinder,} \tag{4.17}$$

$$\Delta\phi = \frac{ml}{G\beta h^3 b} \quad \text{for rectangular parallelepiped,} \tag{4.18}$$

where b is the height of the flexible beam, h is the width of the flexible beam and β is a coefficient related to b and h. Since one has

$$m = k_t \Delta\phi \tag{4.19}$$

hence one can obtain the lumped stiffness k_t of the beam as

$$k_t = \frac{GI}{l} \quad \text{for circular cylinder,} \tag{4.20}$$

$$k_t = \frac{G\beta h^3 b}{l} \quad \text{for rectangular parallelepiped.} \tag{4.21}$$

4.2 Planar Two Degrees of Freedom Parallel Robotic Machine

As shown in Fig. 4.3, we take the case of revolute type into account. A planar two-degree-of-freedom mechanism can be used to position a point on the plane and the Cartesian coordinates associated with this mechanism are the position coordinates of one point of the platform, noted (x, y). Vector θ represents the actuated joint coordinates of the planar parallel mechanism and is defined as $\theta = [\theta_1, \theta_2, \ldots, \theta_n]^{\mathrm{T}}$, where n is the number of degrees of freedom of the mechanism studied, and the only actuated joints are those directly connected to the fixed link [59, 61, 133].

As illustrated in Fig. 4.3, a 2-dof planar parallel mechanism is constructed by four movable links and five revolute joints (noted as O_1 to O_5). The two links – whose length are l_1 and l_3 – are the input links. They are assumed to be flexible beams, and

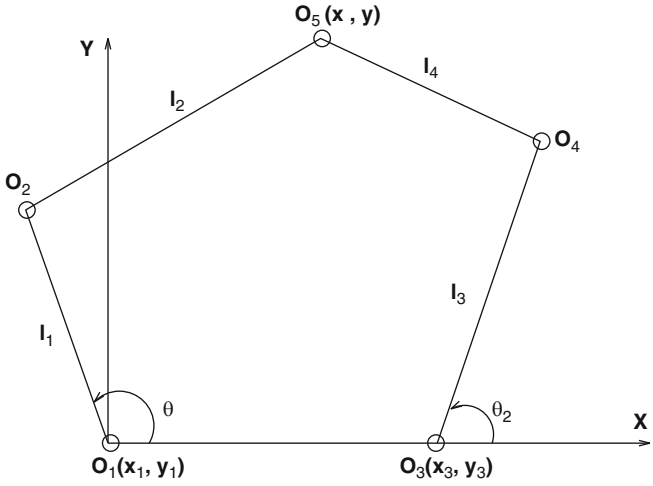

Fig. 4.3 A planar 2-dof parallel mechanism with revolute actuators

points O_1 and O_3 are the only actuated joints in this planar 2-dof parallel mechanism. The lengths of the other two links are denoted as l_2 and l_4, respectively. Point $O_5(x, y)$ is the point to be positioned by the mechanism. The origin of the fixed Cartesian coordinate system is located on joint O_1. (x_1, y_1) and (x_3, y_3) are the coordinates of points O_1 and O_3, respectively, and one has $x_1 = y_1 = y_3 = 0$.

At points O_2 and O_4, one has

$$x_2 = l_1 \cos\theta_1 + x_1, \tag{4.22}$$
$$y_2 = l_1 \sin\theta_1 + y_1, \tag{4.23}$$
$$x_4 = l_3 \cos\theta_2 + x_3, \tag{4.24}$$
$$y_4 = l_3 \sin\theta_2 + y_3. \tag{4.25}$$

From this figure, one obtains

$$l_2^2 = (x - x_2)^2 + (y - y_2)^2, \tag{4.26}$$
$$l_4^2 = (x - x_4)^2 + (y - y_4)^2. \tag{4.27}$$

Substituting (4.22) – (4.25) into (4.26) – (4.27), one gets

$$l_2^2 = (x - l_1 \cos\theta_1)^2 + (y - l_1 \sin\theta_1)^2, \tag{4.28}$$
$$l_4^2 = (x - (l_3 \cos\theta_2 + x_3))^2 + (y - l_3 \sin\theta_2)^2. \tag{4.29}$$

The kinematic relationship can be obtained as follows

$$\mathbf{F}(\theta, \mathbf{p}) = \begin{bmatrix} (x - l_1 \cos\theta_1)^2 + (y - l_1 \sin\theta_1)^2 - l_2^2 \\ (x - (l_3 \cos\theta_2 + x_3))^2 + (y - l_3 \sin\theta_2)^2 - l_4^2 \end{bmatrix} = 0. \tag{4.30}$$

Let

$$\dot{\theta} = \begin{bmatrix} \dot{\theta}_1 \\ \dot{\theta}_2 \end{bmatrix}, \quad \dot{\mathbf{p}} = \begin{bmatrix} \dot{x} \\ \dot{y} \end{bmatrix}. \tag{4.31}$$

One can obtain the Jacobian matrices of the parallel mechanism as

$$\mathbf{A} = \frac{\partial \mathbf{F}}{\partial \mathbf{p}}, \quad \mathbf{B} = \frac{\partial \mathbf{F}}{\partial \theta}. \tag{4.32}$$

In particular, the Jacobian matrices of this planar 2-dof parallel mechanism are as follows:

$$\mathbf{A} = \begin{bmatrix} (x - l_1 \cos\theta_1) & (y - l_1 \sin\theta_1) \\ (x - l_3 \cos\theta_2 - x_3) & (y - l_3 \sin\theta_2) \end{bmatrix}, \tag{4.33}$$

$$\mathbf{B} = \begin{bmatrix} (x \sin\theta_1 - y \cos\theta_1) l_1 & 0 \\ 0 & [(x - x_3) \sin\theta_2 - y \cos\theta_2] l_3 \end{bmatrix}. \tag{4.34}$$

The velocity equations can be written as $\mathbf{A}\dot{\mathbf{p}} + \mathbf{B}\dot{\theta} = 0$ and

$$\mathbf{J} = -\mathbf{B}^{-1}\mathbf{A} = \begin{bmatrix} a_1/d_1 & b_1/d_1 \\ a_2/d_2 & b_2/d_2 \end{bmatrix} \tag{4.35}$$

with

$$a_1 = x - l_1 \cos\theta_1, \tag{4.36}$$
$$a_2 = x - l_3 \cos\theta_2 - x_3, \tag{4.37}$$
$$b_1 = y - l_1 \sin\theta_1, \tag{4.38}$$
$$b_2 = y - l_3 \sin\theta_2, \tag{4.39}$$
$$d_1 = -(x \sin\theta_1 - y \cos\theta_1) l_1, \tag{4.40}$$
$$d_2 = -[(x - x_3) \sin\theta_2 - y \cos\theta_2] l_3. \tag{4.41}$$

In order to compute the Jacobian matrix of (4.35), one has to know the joint angles of Fig. 4.3 first. Therefore, it is necessary to calculate the inverse kinematics of this planar 2-dof parallel mechanism to determine the joint angles for any given end-effector position and orientation. Unlike many serial mechanisms, the calculation of the inverse kinematics of a parallel mechanism is generally straightforward.

From (4.28), one obtains

$$2l_1 x \cos\theta_1 + 2l_1 y \sin\theta_1 = x^2 + y^2 + L_1^2 - L_2^2, \tag{4.42}$$

therefore, one can obtain θ_1 as follow

$$\sin\theta_1 = \frac{BC + K_1 A\sqrt{A^2 + B^2 - C^2}}{A^2 + B^2}, \tag{4.43}$$

$$\cos\theta_1 = \frac{AC - K_1 B\sqrt{A^2 + B^2 - C^2}}{A^2 + B^2}, \tag{4.44}$$

where

$$A = 2l_1 x, \tag{4.45}$$
$$B = 2l_1 y, \tag{4.46}$$
$$C = x^2 + y^2 + L_1^2 - L_2^2, \tag{4.47}$$
$$K_1 = \pm 1 \tag{4.48}$$

and K_1 is the branch index, which can be used to distinguish the four branches of the inverse kinematic problem. In the same way, from (4.29), one obtains

$$2l_3(x - x_3)\cos\theta_2 + 2l_3 y \sin\theta_2 = (x - x_3)^2 + y^2 + l_3^2 - l_4^2. \tag{4.49}$$

Hence one obtains the joint angle θ_2 as

$$\sin\theta_2 = \frac{BC + K_2 A\sqrt{A^2 + B^2 - C^2}}{A^2 + B^2}, \tag{4.50}$$

$$\cos\theta_2 = \frac{AC - K_2 B\sqrt{A^2 + B^2 - C^2}}{A^2 + B^2}, \tag{4.51}$$

where

$$A = 2l_3(x - x_3), \tag{4.52}$$

$$B = 2l_3 y, \tag{4.53}$$

$$C = (x - x_3)^2 + y^2 + l_3^2 - l_4^2, \tag{4.54}$$

$$K_2 = \pm 1. \tag{4.55}$$

Again, K_2 is the branch index.

Assume the actuator stiffnesses of O_1 and O_3 are k_1 and k_1', respectively, and the lumped stiffness for beam O_1O_2 and O_3O_4 are k_b and k_b'. Then the compound stiffness at points O_1 and O_3 are written as

$$k = \frac{k_1 k_\mathrm{b}}{k_1 + k_\mathrm{b}}, \tag{4.56}$$

$$k' = \frac{k_1' k_\mathrm{b}'}{k_1' + k_\mathrm{b}'}, \tag{4.57}$$

where k, k' are the total stiffnesses at the active joint, k_1, k_1' are the actuator stiffnesses and k_b, k_b' are the lumped stiffnesses as indicated in (4.16). One can find the kinetostatic model for this planar 2-dof parallel mechanism by using (4.7), i.e.,

$$\mathbf{K}_\mathrm{C} = \mathbf{J}^\mathrm{T}\mathbf{K}_\mathrm{J}\mathbf{J}, \tag{4.58}$$

where $\mathbf{K_J}$ is the joint stiffness matrix of the parallel mechanism and $\mathbf{J}$ is the Jacobian matrix of this planar 2-dof parallel mechanism.

The analysis described above is now used to obtain the stiffness maps for this planar 2-dof parallel mechanism. The maps are drawn on a section of the workspace of the variation of the end-effector's position.

A program has been written with the software Matlab. Given the values of $l_1 = l_4 = 0.5\,\mathrm{m}$, $l_2 = 0.6\,\mathrm{m}$, $l_3 = 0.8\,\mathrm{m}$, and $O_1O_3 = 0.7\,\mathrm{m}$. The contour graph can be shown in Fig. 4.4.

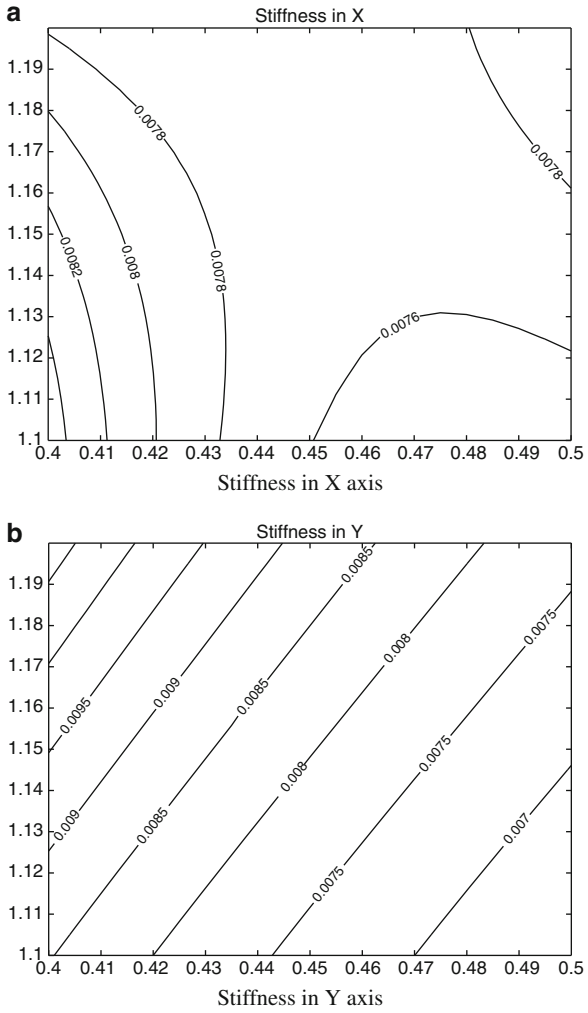

Fig. 4.4 Stiffness contour graph for a planar 2-dof parallel mechanism with revolute actuators

4.3 Planar Three Degrees of Freedom Parallel Robotic Machine

A symmetric mechanism identical to the one studied in [56] and [58] is now analyzed with the procedure described above. The characteristics of this mechanism are as follows: Points A_i, $i = 1, 2, 3$ and points B_i, $i = 1, 2, 3$ (Fig. 4.5) are, respectively, located on the vertices of an equilateral triangle and that the minimum and maximum lengths of each of the legs are the same. The mechanism is therefore completely symmetric. The dimensions and the stiffness of each leg are given in Table 4.2.

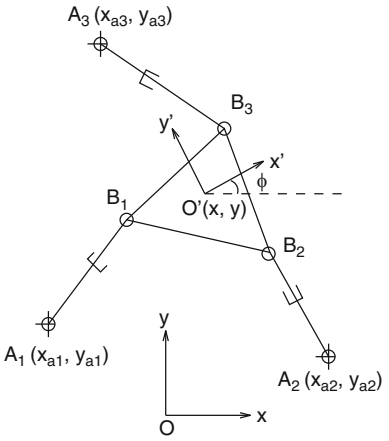

Fig. 4.5 A planar 3-dof parallel mechanism with prismatic actuators

Table 4.2 Geometric properties of symmetric planar parallel mechanism (all length units in mm and stiffness units in N/m)

i	x_{ai}	y_{ai}	x_{bi}	y_{bi}	k_i
1	$-1/2$	$-\sqrt{3}/6$	$-1/12$	$-\sqrt{3}/36$	1,000
2	1/2	$-\sqrt{3}/6$	1/12	$-\sqrt{3}/36$	1,500
3	0	$\sqrt{3}/3$	0	$\sqrt{3}/18$	700

Since one has

$$x_i = x - L\cos\phi_i - x_{ai}, \quad i = 1, 2, 3, \tag{4.59}$$

$$y_i = y - L\sin\phi_i - y_{ai}, \quad i = 1, 2, 3, \tag{4.60}$$

$$p_i = \sqrt{x_i^2 + y_i^2}, \quad i = 1, 2, 3, \tag{4.61}$$

where L is the length of the gripper and p_i is the length of the leg. The Jacobian matrix is given by [56] as follows

$$\mathbf{J} = \begin{bmatrix} a_1/p_1 & b_1/p_1 & c_1/p_1 \\ a_2/p_2 & b_2/p_2 & c_2/p_2 \\ a_3/p_3 & b_3/p_3 & c_3/p_3 \end{bmatrix} \tag{4.62}$$

with

$$a_i = x - x_{ai} - L\cos\phi_i, \tag{4.63}$$

$$b_i = y - y_{ai} - L\sin\phi_i, \tag{4.64}$$

$$c_i = (x - x_{ai})L\sin\phi_i - (y - y_{ai})L\cos\phi_i. \tag{4.65}$$

Hence, according to (4.7), one can find the stiffness model for this planar three-degrees-of-freedom parallel mechanism.

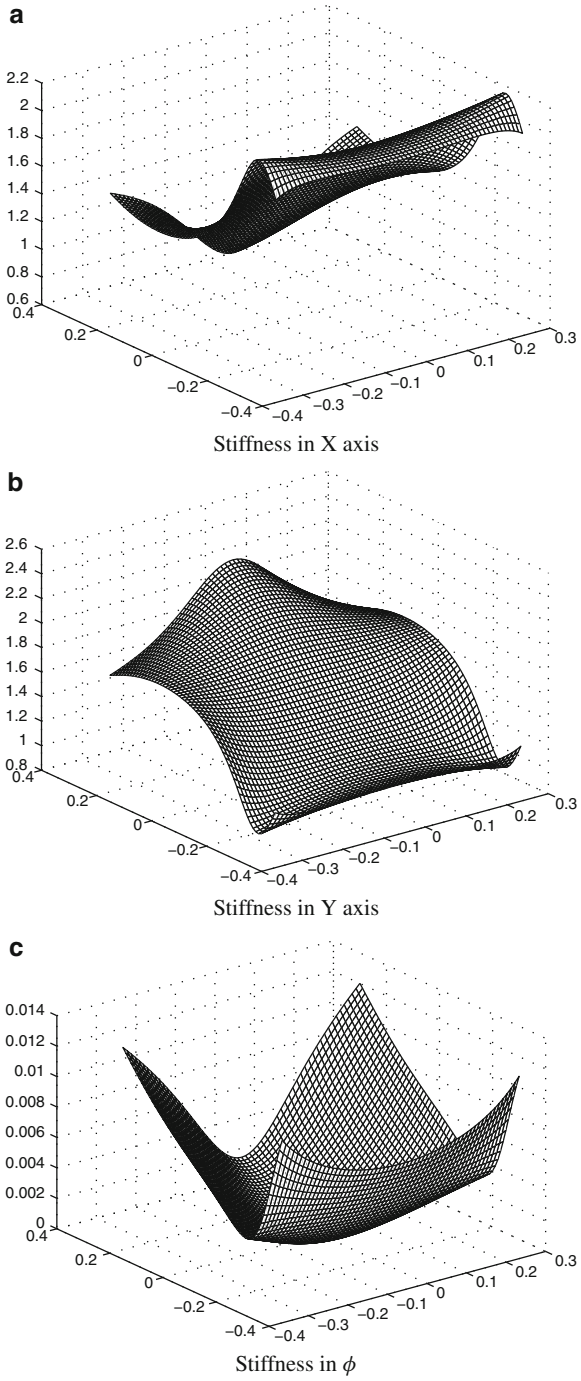

Fig. 4.6 Stiffness mesh graphs for a planar 3-dof parallel mechanism with prismatic actuators ($\phi = 0$)

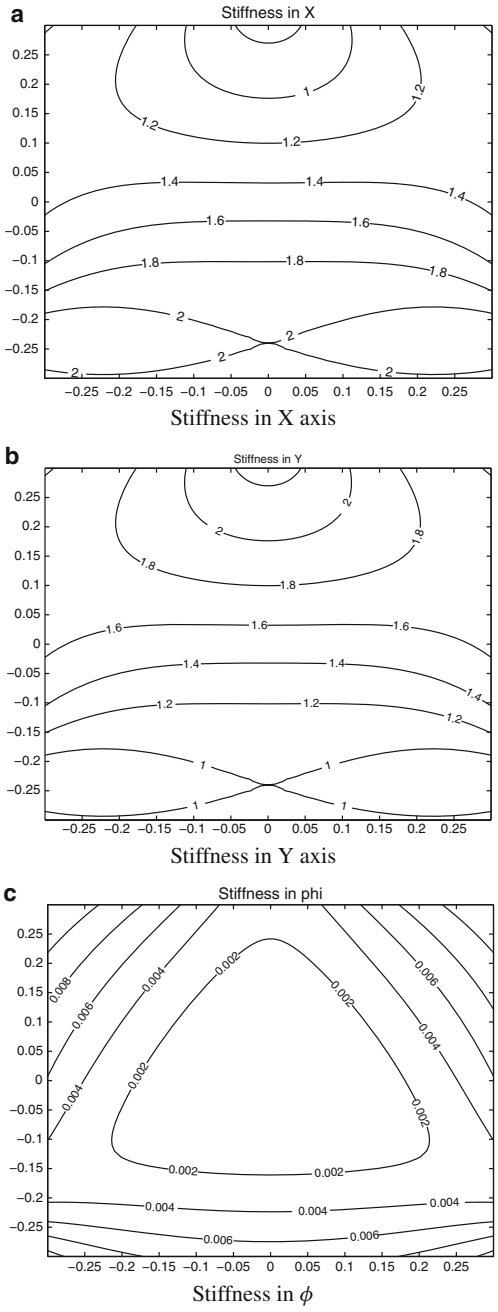

Fig. 4.7 Stiffness contour graphs for a planar 3-dof parallel mechanism with prismatic actuators ($\phi = 0$)

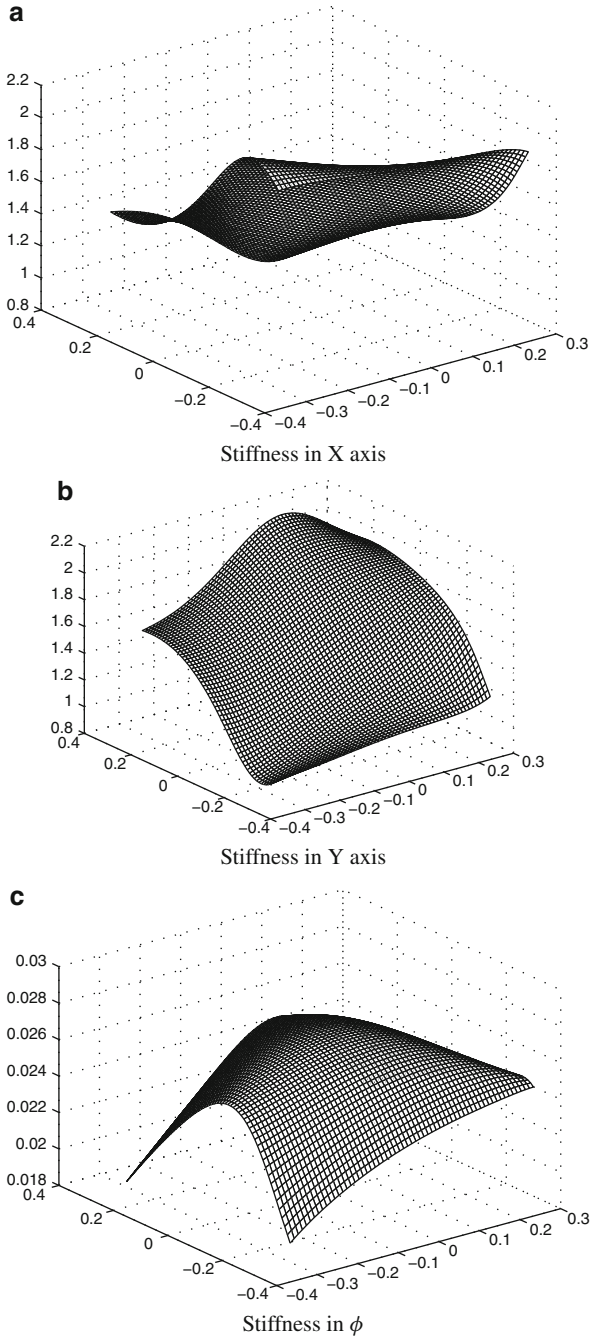

Fig. 4.8 Stiffness mesh graphs for a planar 3-dof parallel mechanism with prismatic actuators ($\phi = \pi/2$)

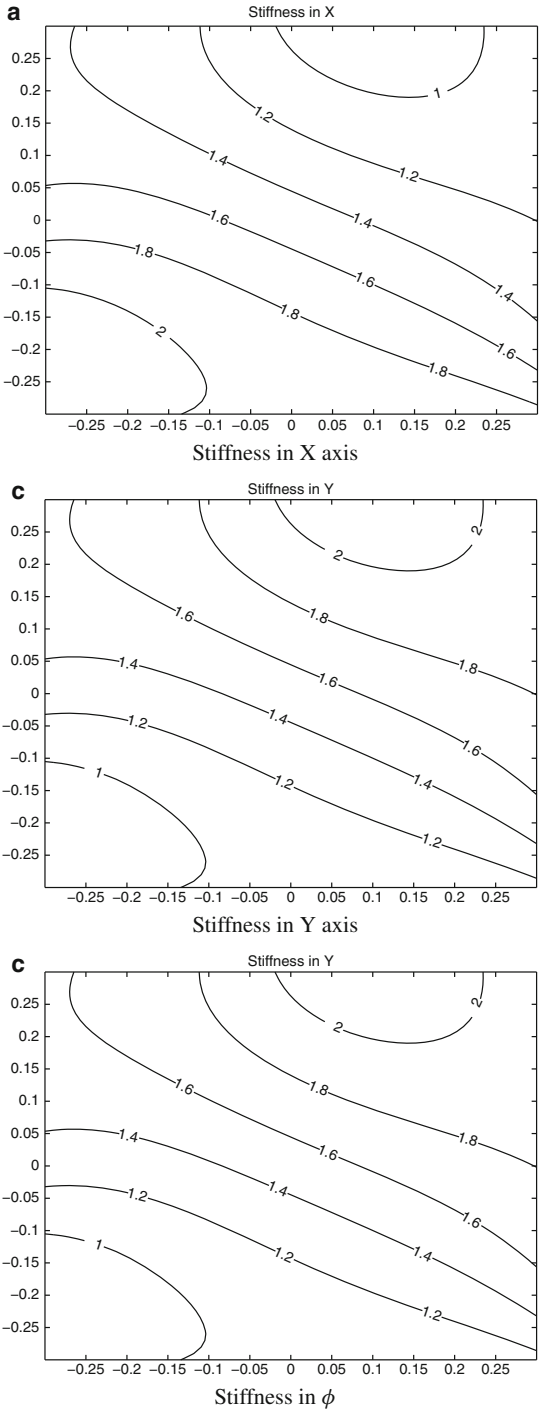

Fig. 4.9 Stiffness contour graphs for a planar 3-dof parallel mechanism with prismatic actuators ($\phi = \pi/2$)

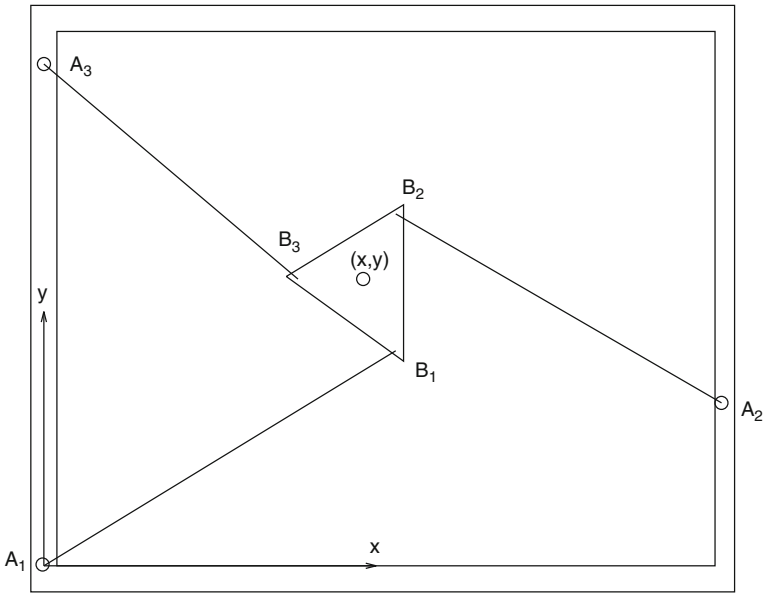

Fig. 4.10 Validation model of the planar 3-dof parallel mechanism in Pro/Motion

Table 4.3 Geometric properties of planar parallel mechanism (all units in mm)

i	x_{ai}	y_{ai}	x_{bi}	y_{bi}	k_i
1	0	0	84.547	48.464	400
2	150	49	84.547	81.536	400
3	0	130	55.91	65	400

The above model is now used to obtain the stiffness maps for this planar 3-dof parallel mechanism. Given the values shown in Table 4.2, one can obtain the stiffness contour and mesh graphs in x, y, and ϕ shown in Figs. 4.6 – 4.9.

One can find from the stiffness map that the symmetric mechanism is in a singular configuration when positioned at the center of the workspace. Also, from such stiffness maps, one can determine which regions of the workspace will satisfy some stiffness criteria. From the mesh graphs, one can view the stiffness distribution more intuitively.

A model (Fig. 4.10) for this planar 3-dof parallel mechanism has been built using the software Pro/Engineer to simulate the physical structure on Pro/Motion.

With the geometric properties given in Table 4.3 and the center of the triangle located at $(75, 65)$, after applying the forces and torque $F_x = 100$ N, $F_y = 100$ N, $\tau = 60$ Nm at the center of the triangle, the three legs deform. One obtains the deformation of the center using Pro/Motion as $\Delta x = 0.09697$ mm, $\Delta y = 0.14959$ mm, $\Delta\phi = -0.0020$. Meanwhile, the results obtained from the equations developed in the previous section are $\Delta x = 0.0962$ mm, $\Delta y = 0.1548$ mm,

$\Delta\phi = -0.0020$. This shows that the results from Pro/Motion and the kinetostatic model are very close to each other.

4.4 Conclusions

A general stiffness model for fully- parallel mechanisms with different actuator stiffnesses has been presented in this chapter. It has been shown that this general stiffness model can be used to evaluate the stiffness properties of parallel mechanisms. Examples have been given to illustrate how this model is used. Meanwhile, the lumped models for joints and links are proposed. They can be applied to establish kinetostatic models for both 2-dof and 3-dof mechanisms which are also mentioned in this chapter. Finally, the reliability of the stiffness model has been demonstrated using the computer program Pro/Engineer.